

IMECE2003-42932

## TWO-COLOR MICRO PIV MEASUREMENTS OF PARTICLE AND FLUID MOTION IN AC ELECTROKINETICS

Dazhi Wang, Carl Meinhart & Marin Sigurdson  
Dept. Mechanical & Environmental Engineering  
University of California at Santa Barbara  
Santa Barbara, CA 93106

### ABSTRACT

Two-Color  $\mu$ -PIV is developed and used to uniquely determine the fluid velocity based on the micron-resolution Particle Image Velocimetry ( $\mu$ -PIV) technique [1-3]. The fluid velocity field was obtained by measuring the motion of two different sizes particles, 0.7 and 1.0  $\mu\text{m}$ . The different sizes of particles contain different fluorescent dyes, allowing them to be distinguished using fluorescent filter cubes. By comparing the velocity fields from the two different size particles, the underlying fluid motion can be uniquely determined, without *a priori* knowledge of the electrical properties of the particles, or the electrical field.

The test section is formed by two wedge-shaped electrodes sandwiched between two glass wafers. In the presence of nonuniform ac electric fields, the particles experience dielectrophoretic (DEP) forces due to polarization and drag forces due to viscous interaction with the suspending medium, and the fluid motion is induced by the electrothermal effect and/or ac electroosmosis. The micro-PIV measurements are used to determine quantitatively the physical characteristics of the AC electrokinetic effects.

### INTRODUCTION

Applying non-uniform electric fields can lead to fluid motion through the electrothermal effect or ac electroosmosis [3-6], which have potential importance in the applications of pumping working liquid in microfluidic devices without moving parts. Spatial variation in the electric field produces non-uniform temperature distributions. The non-uniform temperature field, in turn, causes local changes in conductivity and permittivity. The external electric field interacts with the gradients of the conductivity and permittivity, giving rise to

electrothermal forces in the liquid. In addition, like dc electroosmosis, ac electric fields can also produce fluid motion through ac electroosmosis, which is originated from the action of the non-zero tangential components of the electric fields on the double layers at the interface of the electrodes and the fluid.

In the presence of nonuniform electric fields, particles in a suspension experience dielectrophoretic (DEP) forces [7] as well as drag forces due to fluid motion. The DEP forces cause the particle velocity to be different from the fluid velocity. This force is induced by the difference of polarisability between the particles and the suspending medium, which is a strong function of applied frequency. Many bioparticles, such as cells, viruses, proteins and DNA, can be controlled and separated using DEP forces [8-11].

In this paper, we present a Two-Color  $\mu$ -PIV technique, with which we obtained fluid velocity in a wedge-shaped microchannel. The particle velocity and fluid velocity were compared and analyzed using dielectrophoresis theory.

### THEORY

#### Dielectrophoresis and Particle motion

The DEP force is induced on a particle in an aqueous medium through polarization due to nonuniform electric fields. The time-averaged dielectrophoretic force on a spherical particle is [7]

$$\vec{F}_{DEP} = 2\pi\epsilon_m r^3 \text{Re}\{K\} \nabla |\vec{E}_{rms}|^2 \quad (1)$$

where  $\epsilon_m$  is the permittivity of the medium,  $r$  is the particle radius,  $K$  is the Clausius-Mossotti factor and  $E_{rms}$  is the root mean square of the ac electric field. The real part of  $K$  is denoted by  $\text{Re}\{K\}$ .

The Clausius-Mossotti factor,  $K$ , depends on electrical properties of the particles and the suspending medium, and these properties, in turn, is a function of the frequency of the applied signal.  $\text{Re}\{K\}$  ranges from  $-0.5$  to  $1$ . The DEP force can move a particle to areas of high field if it is positive ( $\text{Re}\{K\} > 0$ ) or low field if it is negative ( $\text{Re}\{K\} < 0$ ).

Under the influence of DEP forces, the particles will not follow the flow faithfully. Therefore, the particles also experience drag forces through viscous interaction with the fluid. The drag force on a spherical particle at zero Reynolds number follows Stokes' law

$$\vec{F}_{DRAG} = 6\pi\mu r(\vec{u}_f - \vec{u}_p) \quad (2)$$

where  $\mu$  is the viscosity of the medium,  $u_f$  is the fluid velocity and  $u_p$  is the particle velocity.

At steady state the dielectrophoretic force and the drag force are balanced by each other. The particle motion is governed by

$$\vec{F}_{DEP} + \vec{F}_{DRAG} = 0. \quad (3)$$

### Electrothermal effect

Nonuniform electric fields dissipate power to the fluid. Assuming temperature convection is negligible compared to conduction, the fluid temperature can be obtained by solving the heat equation at steady state

$$k\nabla^2 T + \sigma E^2 = 0 \quad (4)$$

where  $\sigma$  is the conductivity, and  $\sigma E^2$  represents the power density generated in the fluid by applied electric fields. The electric field can be written as  $E = -\nabla V$ , where  $V$  is the applied voltage.

The temperature field is not uniform since the applied electric fields are not uniform. The spatially varying temperature field causes local changes in conductivity and permittivity. The electric fields interact with the gradients of permittivity and conductivity, giving rise to the electrothermal force that puts the fluid into motion. This phenomenon is termed electrothermal effect. The time-averaged electrothermal force is expressed as [4]

$$\vec{f}_E = -\frac{1}{2} \left[ \left( \frac{\nabla \sigma}{\sigma} - \frac{\nabla \varepsilon}{\varepsilon} \right) \cdot \vec{E}_0 \frac{\varepsilon \vec{E}_0}{1 + (\omega\tau)^2} + \frac{1}{2} |\vec{E}_0|^2 \nabla \varepsilon \right] \quad (5)$$

where  $E_0$  is the amplitude of the applied electric field,  $\omega$  the applied voltage and  $\tau = \varepsilon/\sigma$  is the charge relaxation time. The gradients of conductivity and permittivity are related to temperature by  $\nabla \varepsilon = (\partial \varepsilon / \partial T) \nabla T$  and  $\nabla \sigma = (\partial \sigma / \partial T) \nabla T$ .

### AC electroosmosis

AC electric fields can produce fluid motion like dc electroosmosis [4-6]. After applying the electric fields, the

charges on the surface of the electrodes attract ions of opposite sign in the fluid, giving rise to double layers. The electrical forces due to the non-zero tangential components of the electric fields pull the ions that lie inside the double layer along the electrode surface, resulting in fluid motion through viscous friction.

Assuming that the double layer width is much smaller than the characteristic length of the electrodes and the electric potential is small, the fluid velocity outside the double layer is given by [6]

$$u_f = -\frac{\varepsilon}{4\mu} \Lambda \nabla_s (|\Delta V|^2) \quad (6)$$

where  $\Lambda$  is a factor related to the double layer structure,  $\nabla_s$  represents a gradient across the electrode surface and  $\Delta V$  is the potential drop across the double layer.

### Fluid motion

The motion of incompressible fluid is governed by the Navier-Stokes equation and the mass-conservation equation. In our experiments the fluid velocity is around  $100 \mu\text{m/s}$  and the characteristic length of the electrodes is  $50 \mu\text{m}$ . Therefore the Reynolds number is much less than  $1$  and the inertial terms in the Navier-Stokes equation can be dropped. The governing equations are

$$\mu \nabla^2 \vec{u}_f - \nabla p + \vec{f} = 0 \quad (7)$$

and

$$\nabla \cdot \vec{u}_f = 0, \quad (8)$$

where  $p$  is the pressure and  $f$  is the body force. In our experiments the particle volume fraction is smaller than  $0.1\%$ , so the effect of the particles on the fluid is negligible.

For the electrothermally-induced flow, the fluid velocity can be determined by substituting Eq. (5) into (7), and setting  $f = f_E$ . For ac electroosmosis induced flow, the body force  $f = 0$  at the region outside the doubly layer, and the bulk fluid velocity can be obtained by solving Eq's. (7) and (8) along with the boundary condition described by Eq. (6).

## EXPERIMENTAL METHOD

### Apparatus and Materials

The experiments were conducted using a wedge-shaped microchannel coupled with microelectrodes. The fluid containing fluorescent particles inside the channel was put into motion by ac electric fields, and the images through a microscope were recorded on a CCD camera and analyzed using a PIV software.

Fluorescent polystyrene spherical particles of two different sizes,  $0.7$  and  $1.0$  micron diameters, were suspended in a solution of  $8.5\%$  (w/v) sucrose and  $0.3\%$  (w/v) dextrose. The volume fractions of the  $0.7$  and  $1.0$  micron diameter particles

are 0.05% and 0.02%, respectively, and the total volume fraction of the particles is 0.07%. The Clausius-Mossotti factor  $Re\{K\}$  is  $-0.5$ , therefore dielectrophoresis is negative, which pushes particles away from increasing electric field intensity.

The ac electric fields were provided with a Stabilized Sweep Generator (Model 22, WAVETEK) and a Stereo Power Amplifier (Model P500, David Hafler). A Digital Phosphor Oscilloscope (Model TDS3032, Tektronix) is used to measure the frequency and voltage applied on the microelectrodes. The  $\mu$ -PIV system consists of a microscope and a CCD camera to record particle images. In our experiments we used an Epi-Fluorescence microscope (Model ECLIPSE E600FN, Nikon) and a  $1280 \times 1024 \times 12$ -bit Hamamatsu CCD camera.

### Mirofluidic Device

Figure 1 shows the microfluidic device. Two electrodes, separated by a  $50\mu\text{m}$  gap, are sandwiched between two glass wafers, forming a wedge-shaped  $550\mu\text{m}$  deep microchannel. The electrodes were fabricated by evaporating  $500\text{\AA}$  Ti and  $2000\text{\AA}$  Au on a silicon chip. The fabrication process consisted of PECVD, photolithography, deep RIE and e-beam evaporation. The microfluidic device was made at UCSB's Nanotechnology Facility.

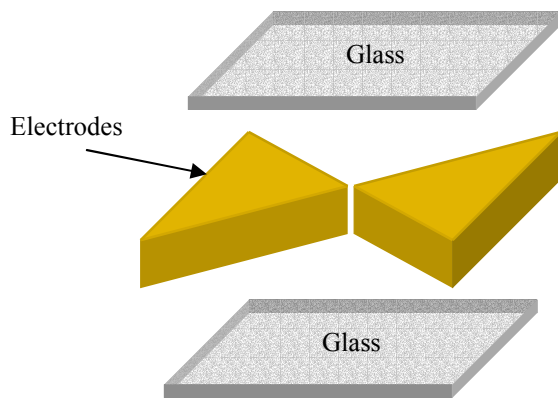


Fig. 1. Schematic diagram of the microfluidic device

The geometry of the channel provides nonuniform electric fields. The region near the electrode apex is of interest where the electric field is strong enough to produce detectable fluid motion and dielectrophoretic forces on particles. Measurements of the particle and fluid motion were obtained on a horizontal plane approximately  $150\mu\text{m}$  beneath the top glass wafer. Due to the high aspect ratio of the depth to the gap ( $550:50$ ), it can be assumed that the electric fields are two-dimensional in the region away from the glass wafers, and therefore the movement of the particles and the fluid are in two-dimension planes.

### Two-Color $\mu$ -PIV

The 2-D fluid motion at the microscale can be measured quantitatively using Micron-resolution Particle Image Velocimetry ( $\mu$ -PIV) technique [1-3]. Small fluorescent spheres were added to the fluid as tracers with the solid volume fraction

less than 0.1%. Images of the particles were recorded continuously on a CCD camera at a constant rate. And then the images on the camera were analyzed with the PIV software to give a 2-D velocity field.

Typically,  $\mu$ -PIV measures the fluid velocity by tracking the motion of fluorescent particles with an assumption that the particles faithfully follow the fluid flow. However in the current experiments, the particle velocity is different from the underlining fluid velocity, due to the DEP forces on the particles induced by the applied electric fields. In order to measure fluid motion subject to nonuniform electric fields, a technique based on  $\mu$ -PIV is developed at UCSB's Microfluidics Laboratory, named Two-Color  $\mu$ -PIV.

The idea is that the fluid velocity can be determined from the velocity fields of two different size particles. Figure 2 schematically shows how to measure the two particle velocity fields using the two-Color  $\mu$ -PIV. The two different size particles were distinguished in PIV measurements by labeling them with different color fluorescent dyes. Both sizes of particles were placed into the microchannel. With the filter cube consisting of the green and red filters, only the larger size particle images were recorded. With the other filter cube consisting of the green and blue filters, only the smaller size particle images were recorded. Therefore, the identical fluid motion is obtained during the measurements.

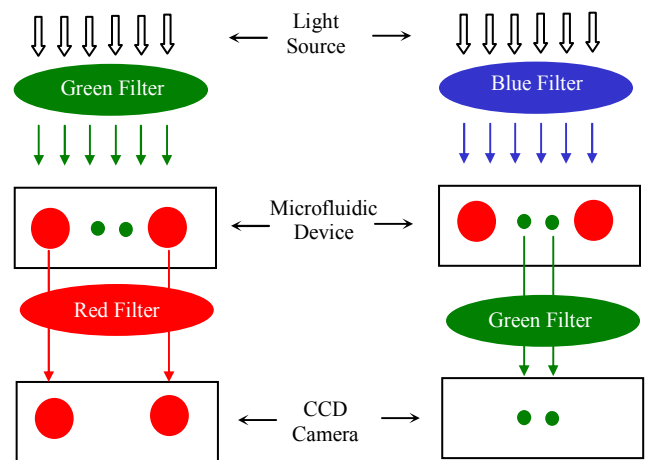


Fig. 2. Schematic of the process of the measurements using two-Color  $\mu$ -PIV. Two PIV measurements can be conducted in one experimental section by switching the color filters.

Equations (1) and (2) indicate that for spherical particles, the magnitude of DEP force scales with radius cube, while the magnitude of the hydrodynamics drag force scales linearly with radius. Plugging these two equations into Eq. (3) and rearranging the terms, the governing equations for two different size particles, with similar electrical properties, are given by

$$\varepsilon_m r_1^2 \operatorname{Re}\{K\} \nabla |\vec{E}_{rms}|^2 + 3\mu(\vec{u}_f - \vec{u}_{p1}) = 0 \quad (9)$$

and

$$\varepsilon_m r_2^2 \operatorname{Re}\{K\} \nabla |\vec{E}_{rms}|^2 + 3\mu(\vec{u}_f - \vec{u}_{p2}) = 0, \quad (10)$$

where  $u_{p1}$  and  $u_{p2}$  are the particle velocity fields, and  $r_1$  and  $r_2$  are the particle radii. The fluid velocity can be derived from the above two equations,

$$\vec{u}_f = \frac{\vec{u}_{p1} r_2^2 - \vec{u}_{p2} r_1^2}{r_2^2 - r_1^2} \quad (11)$$

## RESULTS AND ANALYSIS

AC potential of  $12V_{rms}$  at a frequency of  $200kHz$  was applied to the test suspension wherein there were two different size particles,  $0.7\mu m$  and  $1\mu m$  diameters. The test region is a  $415\mu m \times 415\mu m$  square on a horizontal plane  $150\mu m$  below the top glass cover, corresponding to  $1024 \times 1024$ -bit pixels. The results of the measurements using two-color  $\mu$ -PIV are shown in Fig. 3, including the velocity fields of  $1.0\mu m$  diameter particles (Fig. 3a),  $0.7\mu m$  diameter particles (Fig. 3b) and the fluid (Fig. 3c). Each particle velocity field was obtained by averaging over 90 images taken at a rate of 13 fps. The fluid velocity field was determined from the two particle velocity fields and Eq. (11), without *a priori* knowledge of the 2-D electric field, the fluid properties, or the Clausius-Mossotti factor. The particle velocity fields shown in Fig. 3 are raw data, that is, they are just results of PIV analysis of 90 frames, without applying any smoothing function or data interpolation.

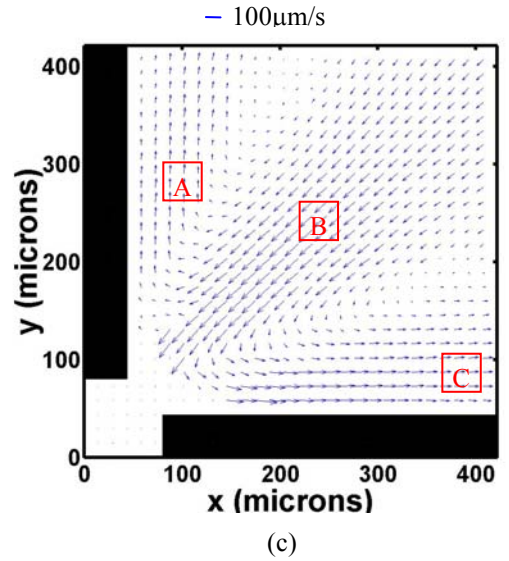
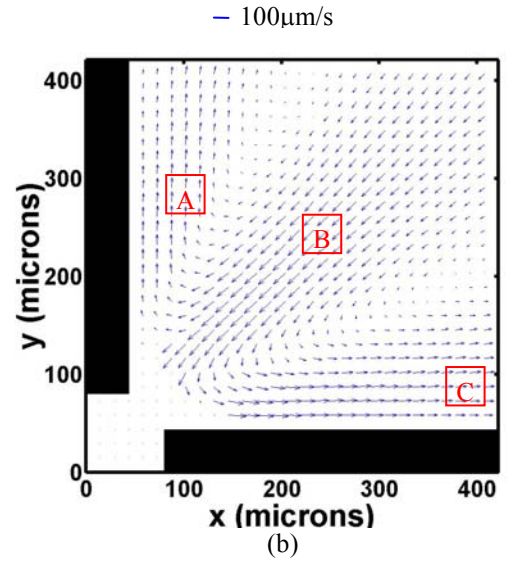
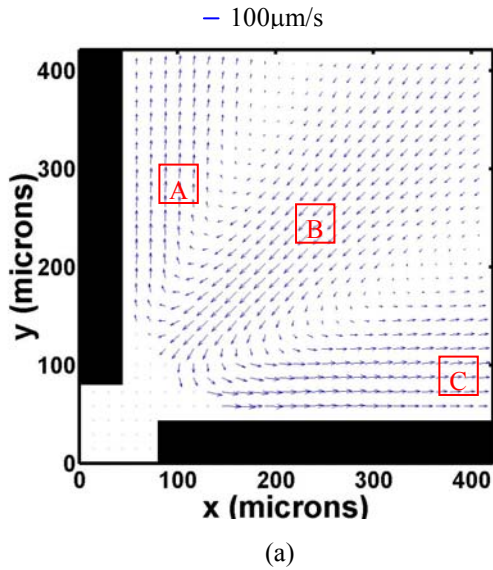


Fig. 3. Particle velocity fields obtained using two-color  $\mu$ -PIV. (a) The velocity of the  $1\mu m$  diameter polystyrene particles; (b) the velocity of the  $0.7\mu m$  diameter polystyrene particles; (c) The fluid velocity field determined from the two particle velocity fields shown in (a) and (b) using Eq. (11). The regions A, B and C are selected to compare the velocity and explain the motion. The black rectangles represent the electrodes. The applied voltage is  $12V_{rms}$  at a frequency of  $200kHz$ . These are raw data, i.e. no smoothing function was applied.

As stated earlier, the particles are influenced by combination of the dielectrophoresis and the fluid flow. Figure 4 shows the negative dielectrophoretic forces on the particles, calculated using finite element simulation. The similarity between the three pictures in Fig. 3 indicates that the influence of the fluid flow on the particles dominates over the dielectrophoresis. Otherwise the particles would have been

moving away from the electrode tips in the directions as shown in Fig. 4.

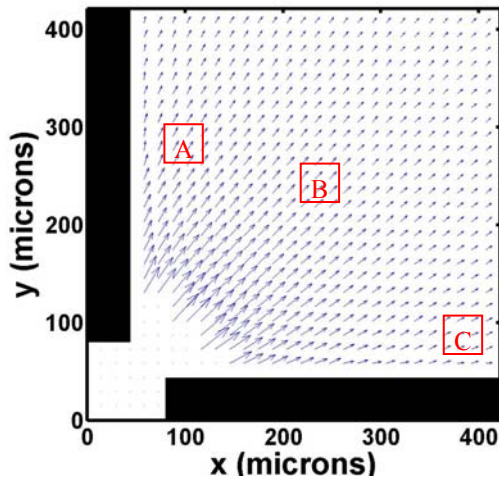


Fig. 4. Numerical simulation of dielectrophoretic forces. They are negative DEP, tending to move the particles away from the electrode tips (the high field). The dielectrophoresis forces near the electrode tips are not given because their magnitudes are too large.

Three regions A, B and C were selected to give a detailed analysis, two near the electrodes, one at the center, as shown in Figs. 3 and 4. The magnitudes of the velocity vectors within each region were averaged and given in Table 1, where  $u_{p1}$  is the velocity of  $1\mu\text{m}$  diameter particles,  $u_{p2}$  the velocity of  $0.7\mu\text{m}$  diameter particles and  $u_f$  the fluid velocity.

Table 1. Micro PIV measurements of velocity in the region depicted in Fig. 3 ( $\mu\text{m/s}$ ).

Region Velocity	A	B	C
$u_{p1}$	65	107	88
$u_{p2}$	59	121	85
$u_f$	54	135	82

At regions A and C, all particles are moving faster than the fluid and the  $1\mu\text{m}$  diameter particles are faster than the  $0.7\mu\text{m}$  diameter, whereas this velocity sequence is reversed at region B. These experimental data can be explained by comparison with dielectrophoresis shown in Fig. 4, and the fluid flow shown in Fig. 3. At regions close to the electrodes, such as A and C, the dielectrophoretic forces are in the same direction as the fluid flow, pointing away from the electrode surfaces, with a tendency to push the particles ahead of the fluid. On the contrary, at areas around the center region, such as B, the dielectrophoretic force tends to push the particles against the fluid flow, giving rise to the observation that the particles are moving slower than the fluid in B. In addition, Eq. (1) indicates the magnitude of the dielectrophoretic force scales with the cube of the particle radius. Therefore the  $1\mu\text{m}$  diameter particles experience three times the dielectrophoretic force as

the  $0.7\mu\text{m}$  diameter particles. Therefore, the velocity of the  $1.0\mu\text{m}$  particles is larger than that of the  $0.7\mu\text{m}$  particles in regions A and C, and the reverse is true for region B.

## CONCLUSION

In the presence of ac electric fields, the detailed 2-D fluid motion in a microsystem was measured using the two-color  $\mu$ -PIV technique. The particle velocity and the fluid velocity were compared quantitatively at several regions. The differences were explained using ac electrokinetic theory. Despite all the differences, the pattern of particle movement is similar to that of the fluid flow, indicating the fluid motion is driven by electrothermal effects or ac electroosmosis, and dominates the overall motion of the particles. However, the effect of dielectrophoresis must be taken into account for accurate fluid velocity measurements.

## ACKNOWLEDGEMENT

This work is supported by DARPA/ARMY DAAD 19-00-1-0400, DARPA/Air Force F30602-00-2-0609, NSF CTS-9874839 and NSF ACI-0086061.

## REFERENCES

- [1] Meinhart, C. D., Wereley, S. T. and Gray, M. H. B., 2000, "Volume illumination for two-dimensional particle image velocimetry", *Measurement Science and Technology*, **11**, pp. 809 - 814.
- [2] Meinhart, C. D. and Wang, D., 2001, "Accurate measurement of dielectrophoretic (DEP) mobility of particles and macromolecules", *Proceedings of  $\mu$ -TAS 2001*, Monterrey, CA.
- [3] Meinhart, C. D., Wang, D., and Turner, K., 2003, "Measurement of Ac Electrokinetic Flows", *Biomedical Microdevices*, **5**, pp. 139-145.
- [4] Ramos, A., Morgan, H., Green, N. G., and Castellanos, A., 1998, "Ac electrokinetics: a review of forces in microelectrode structures", *Journal of Physics D: Applied Physics*, **31**, pp. 2338-2353.
- [5] Green, N. G., Ramos, A., Gonzalez, A., Morgan, H. and Castellanos, A., 2000, "Fluid flow induced by nonuniform ac electric fields in electrolytes on microelectrodes-I. Experimental measurements", *Physical Review E*, **61**, pp. 4011-4018.
- [6] Ramos, A., Gonzalez, A., Green, N. G., Castellanos, A. and Morgan, H., 2000, "Fluid flow induced by nonuniform ac electric fields in electrolytes on microelectrodes-II. A linear double-layer analysis", *Physical Review E*, Vol. 61, No. 4, pp.4019-4028.
- [7] Jones, T., 1995, *Electromechanics of particles*, Cambridge University Press, New York.
- [8] Bakewell, D. J. G., Hughes, M. P., Milner, J. J. and Morgan, H., 1998, "Dielectrophoretic manipulation of avidin and DNA", *Proceedings of the 20<sup>th</sup> Annual International Conference of the IEEE Engineering in Medicine and Biology Society*, **20**, pp. 1079-1082.
- [9] Morgan, H., Hughes, M. P. and Green, N. G., 1999, "Separation of submicron bioparticles by dielectrophoresis", *Biophysical Journal*, **77**, pp. 516-525.

- [10] Yang, J., Huang, Y., Wang, X.-B., Becker, F. F. and Gascoyne, P. R. C., 1999, "Cell Separation on Microfabricated Electrodes Using Dielectrophoretic/Gravitational Field-Flow Fractionation", *Analytical Chemistry*, **71**, pp. 911-918.
- [11] Sigurdson, M., Meinhart, C. D., Wang, D., Lui, X., Feng, J., Krishnamoorthy, S. and Makhijani, V.B., 2002, "Transport Enhancement in Tunable Laser Cavity Sensor", ASME – IMECE'02 MEMS Symposium, New Orleans, LA.